Received: 5 March 2019 | Revised: 3 July 2019 | Accepted: 30 August 2019

DOI: 10.1002/we.2423

RESEARCH ARTICLE

WILEY

An engineering condition indicator for condition monitoring of wind turbine bearings

Aijun Hu | Ling Xiang | Lijia Zhu

Department of Mechanical Engineering, North China Electric Power University, Beijing, China

Correspondence
Hu Aijun, Department of Mechanical Engineering, North China Electric Power University, Beijing 071003, China.
Email: bdlaohu@126.com

Funding information
National Natural Science Foundation of China, Grant/Award Numbers: 51475164 and 51675178

Abstract

Condition monitoring (CM) of wind turbine becomes significantly important part of wind farms in order to cut down operation and maintenance costs. The large amount of CM system vibration data collected from wind turbines are posing challenges to operators in signal processing. It is crucial to design sensitive and reliable condition indicator (CI) in wind turbine CM system. Bearing plays an important role in wind turbine because of its high impact on downtime and component replacement. CIs for wind turbine bearing monitoring are reviewed in the paper, and the advantages and disadvantages of these indicators are discussed in detail. A new engineering CI (ECI), which combined the energy and kurtosis representation of the vibration signal, is proposed to meet the requirement of easy applicability and early detection in wind turbine bearing monitoring. The quantitative threshold setting method of the ECI is provided for wind turbine CM practice. The bearing run-to-failure experiment data analysis demonstrates that ECI can evaluate the overall condition and is sensitive to incipient fault of bearing. The effectiveness in engineering of ECI is validated though a certain amount of real-world wind turbine generator and gearbox bearing vibration data.

KEYWORDS

bearing, condition monitoring, fault detection, indicator, wind turbine

1 | INTRODUCTION

Wind energy is currently the fastest-growing type of renewable energy resource in the world. According to the statistical data by World Wind Energy Association (WWEA), the total global installed wind capacity had reached 435 GW by the end of 2015. The global growth rate of 17.2% in 2015 was higher than in 2014 (16.4%). And China's total installed wind capacity had reached around 148 GW, adding 33 GW of new capacity.[1] It is estimated that by 2020, wind power could supply 2.600 TWh, about 11.5% to 12.3% of global electricity supply, rising to 21.8% by 2030.[2] However, the industry still experiences premature component failures, which increase operation and maintenance (O&M) costs.[3,4] For example, for a 20-year life turbine, the (O&M) costs of 750 kW turbines may constitute about 25% to 30% of the total generation cost or 75% to 90% of the vestment costs. And the O&M costs for 2-MW-type turbine might be 12% less than an equivalent project of 750-kW machines.[5,6] At the same time, as turbines are installed offshore, these failures will become even more costly. General Electric (GE) Energy quoted that a $5000 bearing replacement task can easily turn into a $250 000 project involving cranes, service crew, gearbox replacements, and generator rewinds without mentioning the downtime loss of power generation.[7] Therefore, research on fault diagnosis and condition monitoring (CM) of wind turbine becomes significantly important part of wind farms in order to cut down O&M costs.

CM is a method to assess a system's health, which enables proactive maintenance planning, reduces downtime and operations and maintenance costs, and, to some extent, increases safety. There are a few literature reviews on wind turbine CM,[4-11] and future research is needed because of the importance of CM in wind turbines.[7]

The public surveys show that the gearbox exhibits the highest downtime per failure among all onshore wind turbine sub-assemblies,[12] and the gearbox alone could be responsible for up to one third of all lost wind turbine availability.[13] In additional, it is pointed out that bearings cause more than 50% of faults on gearboxes.[4] The investigation based on operating data of nine wind farms in northern China and a total of 417 wind turbines shows that the generator bearing failure accounted for 67.14% of the total failure in the wind turbine drivetrain.[14] The CM methods of wind turbine drivetrain are briefly discussed in the following.

Various methods have been applied in CM of wind turbines such as vibration analysis,[3,8,15-17] oil debris analysis,[18] sound-aided analysis,[19] and supervisory control and data acquisition (SCADA) data analysis.[20,21] The advantage and disadvantage of the existing wind turbine CM methods are analyzed from the aspect of technical and commercial challenges.[4,9] It is pointed out that oil analysis is valuable for gearbox monitoring. However, it is costly online, so it is likely to be used in future offline.[9] Acoustic emissions could be helpful for detecting drivetrain, blade, or tower defects but are wide bandwidth and costly to both measure and analyze. The SCADA-based wind turbine CM system is cost-effective, because it uses data already being collected at the wind turbine controller. Although some commercial SCADA-based wind turbine CM systems have been developed, it cannot replace a professional purpose-designed wind turbine CM system at the moment.[9] One of the most important reasons is that the SCADA data are collected at a low sampling frequency, which is considered too low for some CM systems and accurate fault diagnosis. Therefore, vibration analysis continues to be "the most popular technology employed in wind turbine, especially for rotating equipment."[5,22]

Considering the time-varying operational conditions applied to wind turbines, besides the conventional spectral analyses, many advanced signal processing techniques[9,23-25] have been developed for interpreting the nonlinear and nonstationary vibration signals collected from the turbines. Typical vibration monitoring sampling rates are around 10 to 20 kHz.[8] The large amount of CM system data collected from wind turbines is posing challenges to operators in signal processing. Some CM systems transmit raw vibration signals for offline analysis in the operator database. However, it claims that a more common and lower-bandwidth approach is to analyze vibration signals locally in the wind turbine CM systems and only convey the resultant spectra or minute-averaged trends to the operator database.[8] Usually, further analyses or advanced signal processing techniques are implemented only when CM settings detect an unusual condition. It is indicated that if there are several wind turbines near but under the alarm level, the O&M will not be notified until the threshold is passed.[4] Therefore, it is crucial to design sensitive and reliable condition indicator (CI) in wind turbine CM system.

CIs are designed to describe the time or frequency domain signal waveform or analysis result from specific analysis algorithm in a statistical manner.[26] Statistical features such as root mean square (RMS), peak, peak to peak, kurtosis, and crest factor (CF) are widely used for the wind turbine fault diagnosis,[5,8,26] but more advanced features are also being developed.[5,8,27] The properties of the common CIs are discussed in detail.[26-30]

Form current literatures, most CIs in wind turbine suffer from two main defects. First, some indicators (RMS, peak, kurtosis, etc) are easy to calculate but less sensitive, at the same time; the TSA, residual, or difference signal–based indicators are too complex to implement for CM system in field application because of the complex structure and time-varying rotating speed of wind turbine. Second, it is difficult to set unified alarm threshold. Some CIs can be set definite threshold in wind turbine monitoring. For example, VDI 3834 defines RMS threshold of vibration velocity and acceleration for the drivetrain components and nacelle and widely adopted by the wind farm operator. However, many CIs indicate the wind turbine condition through relative value and health baseline threshold is needed sometimes.[3] It is difficult to generalize these CIs in different wind farms because of the lack of unified quantitative standards.

And the CIs that indicate the wind turbine condition through relative value are difficult to generalize in different wind farms.

Azevedo et al[4] concluded five main challenges that enclose technical, financial, operational, and management issues from CM system purchase up to the wind farm monitoring stage. Easy automatization, applicability, and early detection are the main technical challenges in wind turbine monitoring. And wind turbine bearing monitoring is highlighted because of its high impact on downtime and component replacement.

Based on the property analysis of main CIs applied in wind turbines, a new engineering CI (ECI) for CM of wind turbine bearings is proposed. The effectiveness of the ECI is validated though bearing run-to-failure experiment and field vibration test of wind turbines. The threshold setting method of ECI is provided for wind turbine CM practice.

The paper is organized as follows. CIs in wind turbine bearing monitoring are reviewed, and the advantages and disadvantages of these indicators are discussed in Section 2. The ECI for CM of wind turbine bearings is proposed in Section 3. In Section 4, the proposed approach is verified using the bearing run-to-failure experiment data. After that, the fifth session presents case studies of field wind turbine bearing fault detection using ECI to demonstrate the effectiveness. The last section provides remarks and conclusions.

2 | REVIEW OF CIs IN WIND TURBINE BEARING MONITORING

There are many statistical features in time-domain and frequency domain of vibrations that have been employed as CIs for wind turbine bearing health. The description and mathematical interpretation of main CIs for wind turbine bearing are provided in this section. The effectiveness (advantages and disadvantages) of the indicators is also discussed.

2.1 | Root mean square

RMS represents the effective value (magnitude) of the vibration signal. RMS is defined as the square root of the average of the sum of the squares of the signal samples.

$$\mathrm{RMS} = \frac{1}{N}\sqrt{\sum_{i=1}^{N}(x_i)^2}, \tag{1}$$

where x_i is the is the ith member of the original sampled time signal and N is the number of samples.

RMS values of vibration signals are used to evaluate the overall condition of the mechanical components.[26] This is because the overall vibration level typically increases as the components, gearbox, and bearing, for instance, deteriorate.

However, two known issues have been identified in literature. First, it is not very sensitive to incipient fault.[30] Second, RMS values are also not significantly affected by short bursts of low-intensity vibrations and as a result encounter problems in detecting early stages of bearing failure.[27]

2.2 | Delta RMS

Delta RMS is the difference between two consecutive RMS values. Similar to RMS, delta RMS is used to estimate the general fault progression.[28] If the damage occurs, there will be a more rapid increase in vibration level than the case without damage.[30] The parameter can be estimated using the following equation:

$$\Delta\mathrm{RMS} = \mathrm{RMS}_{i+1} - \mathrm{RMS}_i. \tag{2}$$

The disadvantage of this method is that the parameter is very sensitive to load changes[30]; therefore, it is not very suitable for setting alarm levels.[27]

2.3 | Peak and peak to peak

Peak is the maximum amplitude value of the sampled vibration signals. Peak-to-peak value is the distance between the maximum amplitude and the minimum amplitude of the sampled vibration signal. Compared with peak-to-peak value, peak value is usually not used very often.[26]

Peak or peak-to-peak value may indicate the presence of a defect even at the initial stage; however, the signal source is unknown, and it may create a false alarm.[31]

2.4 | Kurtosis

The kurtosis is the fourth normalized moment of a given signal, which provides a measure of the peakedness of the signal, ie, the number and amplitude of peaks present in the signal. It is given by

$$\mathrm{Kurtosis} = \frac{N\sum_{i=1}^{N}(x_i-\bar{x})^4}{\left[\sum_{i=1}^{N}(x_i-\bar{x})^2\right]^2}, \tag{3}$$

where $\bar{x}$ is the mean value of the signal.

The kurtosis can be seen as the deviation from the standard probability distribution of a real valued random variable. A signal consisting exclusively of Gaussian noise will have a kurtosis of approximately three. In the case of a healthy bearing, white noise is expected with a normal Gaussian distribution. A signal having relatively flat peaks has kurtosis less than three. A signal with more and sharper peaks has kurtosis greater than three.[26] For example, the kurtosis of a double exponential distribution is 5.9. A fault introduces specific components that depart from the normal distribution, thus increasing the kurtosis value.[32]

2.5 | Crest factor

CF is the ratio between the maximum peak and the RMS of the vibration signal.

$$\mathrm{CF} = \frac{\mathrm{Peak}}{\mathrm{RMS}}. \tag{4}$$

The CF states the significance of impulsive phenomena with respect to the RMS value of the signal. CF value is normally between 2 and 6. A CF value over 6 indicates possible machine failure.[26]

Kurtosis and CF are independent of the actual amplitude of the vibration level and measures of the spikiness of the vibration signal. They are of low sensitivity to the variations of load and speed; therefore, they are well suited for detecting a defect at the initial stage.[31] However, as the damage increases, the values of kurtosis and CF come down to more normal bearing like levels. Thus, the kurtosis and CF lack the ability to detect the fault at the later stages.[31,33]

2.6 | Skewness

Skewness is a measure of the asymmetry of the probability density function of the amplitude of a time series. A time series with normal distribution has a skewness of zero. Skewness is calculated using following equation:

$$\text{Skewness} = \frac{N\sum_{i=1}^{N}(x_i-\bar{x})^3}{\left[\sqrt{\sum_{i=1}^{N}(x_i-\bar{x})^2}\right]^3}. \tag{5}$$

The skewness value of a signal with many small values and few large values is positive. The skewness value of a signal with many large values and few small values is negative. The skewness is often combined with other CIs in bearing or gear fault diagnosis systems.

2.7 | Energy-based bearing CIs

Four energy CIs for bearings, which are named ball energy, cage energy, inner race energy, and outer race energy, are reviewed.[26] These four CIs represent the energy of the bearing vibration signal at/around the rolling element fault frequency. A window of observation is usually set around the bearing defect characteristic frequency of different bearing components. Energy-based bearing CIs are calculated using following equation:

$$\text{Energy}_j = \sqrt{\frac{1}{N}\sum_{i=1}^{N}\left(f_j \pm N\right)^2}, \tag{6}$$

where f_j is the bearing defect characteristic frequency of ball, cage, inner race, or outer race. N is half of the window of observation.

The main difficulty of the energy-based bearing CIs in application is their many different bearings in wind turbine generator and gearbox; therefore, it is complicated to calculate these CIs, and sometimes, the bearing defect characteristic frequencies of different bearings are very close. Besides, health baseline thresholds are often needed in such energy-based CIs field application.[3]

2.8 | TALAF

The TALAF bearing fault indicator is the combination of kurtosis and RMS, defined as[34]

$$\text{TALAF} = \log\left(\text{kurtosis} + \frac{\text{RMS}}{\text{RMS}_0}\right), \tag{7}$$

where RMS_0 is the RMS value of a healthy bearing.

The TALAF value constantly increases with the bearing defect dimension, and different degradation levels can be indicated by the TALAF value. But the initial RMS of healthy bearing is needed in application, and this CI has no physical meaning.[31]

3 | PROPOSED ECI

From the review and analysis of current CIs in wind turbine bearing, it is concluded that the absolute threshold value of RMS, kurtosis, and CF can be easily set in wind turbine CM. Considering that the RMS increases with the fault degradation and that the kurtosis is suited for early fault detection, and according to the analysis results of the actual generator bearing data, a new ECI for CM of wind turbine bearings is proposed, and it is defined as

$$\text{ECI} = \frac{N\sum_{i=1}^{N}(x_i-\bar{x})^4}{\sum_{i=1}^{N}(x_i-\bar{x})^2}. \tag{8}$$

Referring to the definition of kurtosis, Equation (8) can be rewritten in the following form:

$$\mathrm{ECI} = \mathrm{Kurtosis}\cdot\sum_{i=1}^{N}(x_i-\bar{x})^2 = \mathrm{Kurtosis}\cdot\sigma^2, \tag{9}$$

where σ is the standard deviation.

Equation (9) shows that the ECI is actually defined as the product of the variance and kurtosis of the vibration signal. Vibration signals are generally expected to be zero mean; therefore, if the mean value is subtracted from the sampled vibration signal, the ECI is calculated as

$$\mathrm{ECI} = \mathrm{Kurtosis}\cdot\mathrm{RMS}^2. \tag{10}$$

From Equation (10), the combination of energy and kurtosis of the vibration is represented by ECI. At the same time, the alarm levels of ECI can be set by RMS and kurtosis referring to the existing standard in application.

4 | EXPERIMENT DATA ANALYSIS

The bearing run-to-failure data,[35] which are generated by the NSF I/UCR Center for Intelligent Maintenance Systems, University of Cincinnati, are used to verify the effectiveness of the proposed ECI. Four Rexnord ZA-2115 double-row bearings were installed on the bearing test rig. Bearing run-to-failure tests are performed under normal load conditions. At the end of the test-to-failure experiment, outer race failure occurred in bearing 1. The ball pass frequency of the outer race (BPFO) is 236.4 Hz. More detailed information about this experiment can be found in the literature.[35]

A total of 984 data files are supplied in the experiment. It is reported that the abnormal health condition can be detected at file number 703 by kurtosis and RMS of the original vibration signals.[36]

The kurtosis of the vibration signal collected at bearing 1 for the entire life cycle is plotted in Figure 1. It can be seen that the kurtosis of the vibration signal is greater than 4.0 from file number 648 and greater than 5.0 from file number 703. This section is the early stage of the damage propagating process in the bearing entire life cycle. The average kurtosis of the first 500 files is calculated as 3.42 and plotted in the red line in the figure, which indicates the health condition of the bearing. At the last stage of the experiment, the kurtosis decreased under the average kurtosis value; thus, the fault at the later stages cannot be detected by the kurtosis.

The proposed ECI result of the bearing run-to-failure data is shown as Figure 2. The average ECI of the first 500 files is plotted in the red line in the figure. It indicates that all of the ECI values of the bearing fault stage are above the red line (health condition), and the ECI increases in relative large values corresponding to the severity of damage.

The ECI of the vibration data between the file numbers 450 to 750 is plotted in Figure 3. It is clearly observed that the ECI value is increased at file number 533. The average ECI value of the first 500 files is 0.02038 g; therefore, the ECI value of the health bearing is decided. The ECI value of file number 533 is 0.0237 g, which is increased by 16.3% compared with that of the health bearing. In addition, the RMS for the entire life cycle is also plotted. The trend of the curve is similar to that in Figure 2. But the kurtosis curve gets better resolution because of the square operation of RMS values.

The actual outer race fault frequency[26] of 230.7 Hz is prominent in the envelop spectrum of file 533 (Figure 4). The early outer race fault is detected.

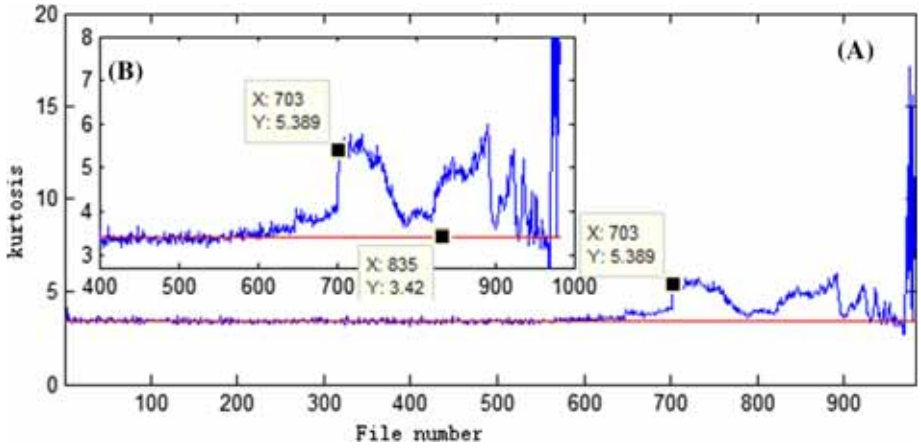

FIGURE 1 Kurtosis of the bearing life cycle vibration signal: (a) kurtosis and (b) local zoom in of the kurtosis from file number 400 [Colour figure can be viewed at wileyonlinelibrary.com]

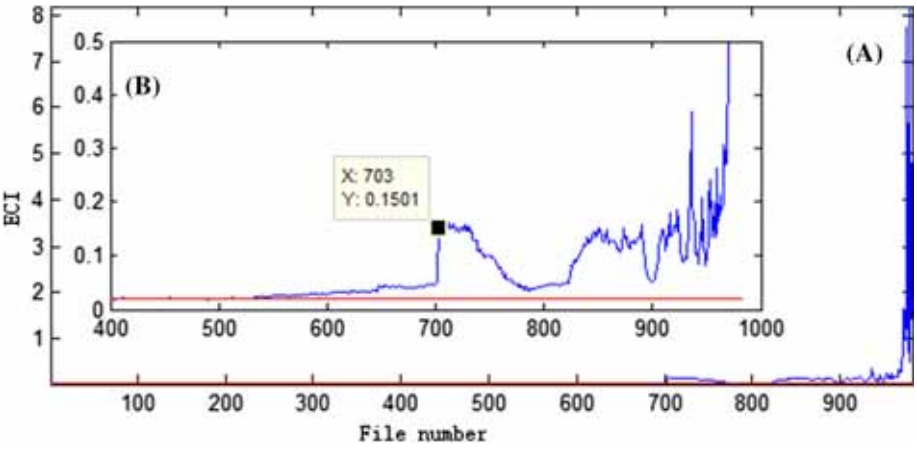

FIGURE 2 Engineering condition indicator (ECI) of the bearing life cycle vibration signal: (a) ECI and (b) local zoom in of the ECI from file number 400 [Colour figure can be viewed at wileyonlinelibrary.com]

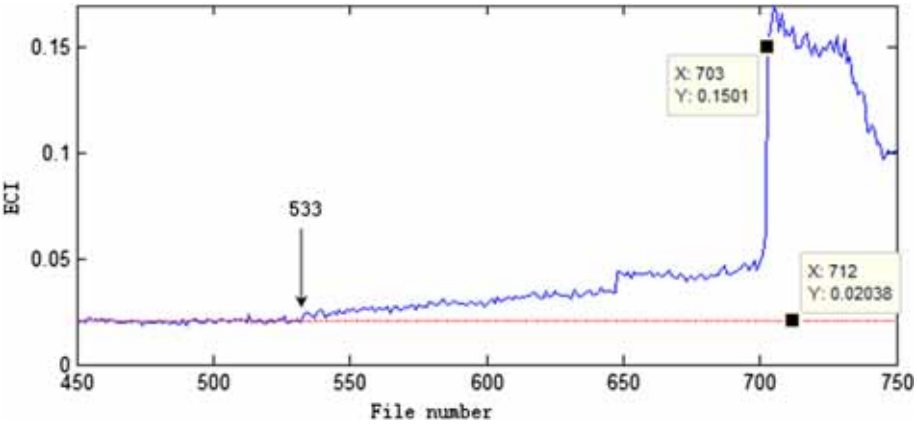

FIGURE 3 Engineering condition indicator (ECI) of the vibration data of file numbers 450 to 750 [Colour figure can be viewed at wileyonlinelibrary.com]

The bearing run-to-failure data analysis result shows that the ECI can well represent the trend of the bearing damage propagating process and detect the bearing fault at its early stage. It is noted that the ECI value of the last two files supplied by the experiment is 0. However, the kurtosis of the last two files is 6.63 and 1.39. Further analysis indicates that only a random impulsive signal with very low amplitude is included in the two

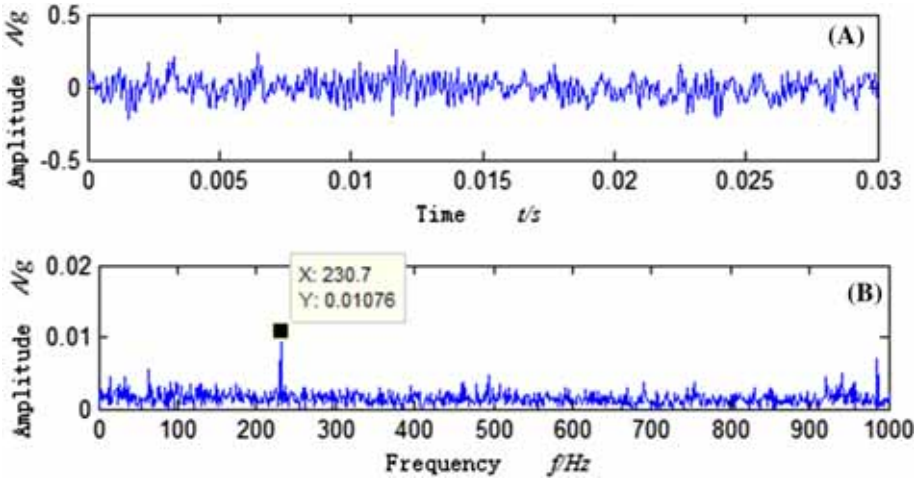

FIGURE 4 Analysis result of early outer race fault (file number 533): A, time waveform; B, envelope spectrum [Colour figure can be viewed at wileyonlinelibrary.com]

files. It means that the bearing test rig is shut down at this moment. Therefore, the data supplied by the last two files in experiment cannot be used in the analysis. It demonstrates the accuracy of ECI in the other aspects.

5 | APPLICATION OF ECI IN WIND TURBINE

Alarm threshold setting is important in CM application. The goal for setting thresholds to indicate drivetrain health is to provide the minimum number of false alarms while maintaining sensitivity to component damage. Usually, further analyses or advanced signal processing techniques are implemented only when the threshold is passed. In this section, real-world wind turbine vibration test data are adopted to evaluate the effectiveness of ECI in engineering.

The field vibration test is performed in a wind farm in North China. A total of 33 1.5-MW doubly fed induction generator (DFIG) onshore wind turbines are installed in the farm. There are no vibration CM systems installed on the wind turbine. The vibration test is performed in the nacelle with Zonic portable vibration analyzer. PCB accelerometers are mounted on bearing housing of the drive end and non–drive end bearing. The vertical direction vibration signal at running speed are recorded. Each recorded dataset consists of 2-minute vibration signal. The sampling frequency is set to 12 800 Hz. Two bearing types, SKF6330C3/VL2071 and SKF6332M/C3, are tested. Vibration data of 19 generator bearings are collected in this test.

5.1 | Threshold setting

According to VDI 3834, the acceleration warning and alarm limits guide value of generator in RMS are 10 and 16 m/ss, respectively. The wind farm has no vibration online monitoring system and vibration history record. For this condition, it is recommended that the initial values for the warning limits should be based on either experience or similar turbines, and the warning limits should not be set higher than 1.25 times the upper limit. The maintenance company of the wind farm suggested that the RMS band limits are set to 12.5 and 20 m/ss on the basis of similar turbines of other wind farm. These limits are adopted in ECI threshold calculation. Usually, kurtosis of the healthy bearing is about 3. Considering the average kurtosis of the run-to-failure bearing in healthy stage is 3.42 (Figure 1) and most of the kurtosis of the generator bearing field test vibration signal is less than 4.0, the kurtosis limit is set to 4.0 in ECI threshold calculation. Thus, the warning and alarm limits of ECI are set according to Equation (10).

5.2 | Application in generator bearing

The RMS, kurtosis, and CF are analyzed first to evaluate their performance in wind turbine CM. The results are shown in Figures 5–7. Figure 5 depicts the RMS bar chart of the tested bearings. Bar color is displayed in yellow or red, while the RMS value is greater than the warning or alarm limits. It can be seen that three bearings are in alarm band and four bearings are in warning band.

Bar color is displayed in red if the kurtosis is greater than 4.0 in Figure 6. It shows four bearings are regarded as abnormal health condition. Kurtosis of other bearings is less than 4.0. It is noted that bearing number 9 has relative high kurtosis but low RMS value, which means bearing

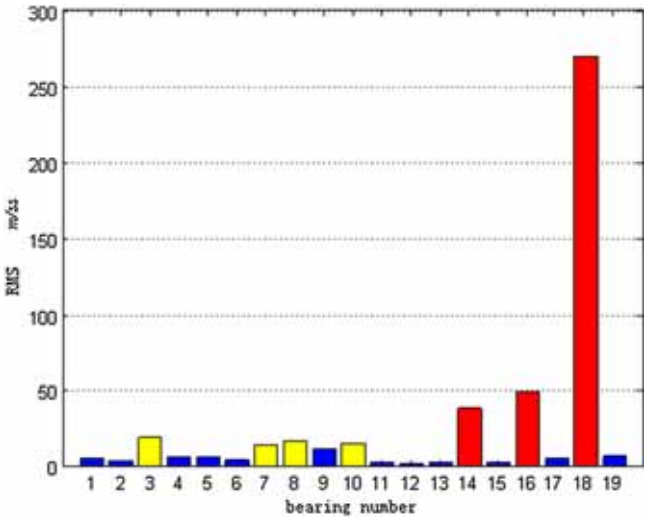

FIGURE 5 Root mean square (RMS) of the generator bearing vibration signal [Colour figure can be viewed at wileyonlinelibrary.com]

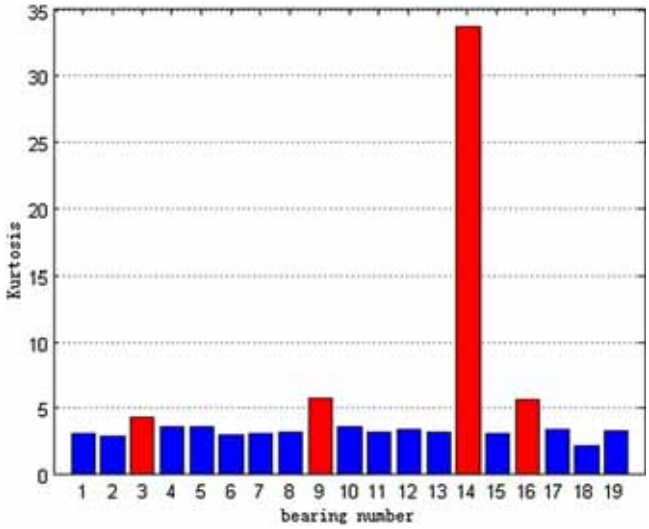

FIGURE 6 Kurtosis of the generator bearing vibration signal [Colour figure can be viewed at wileyonlinelibrary.com]

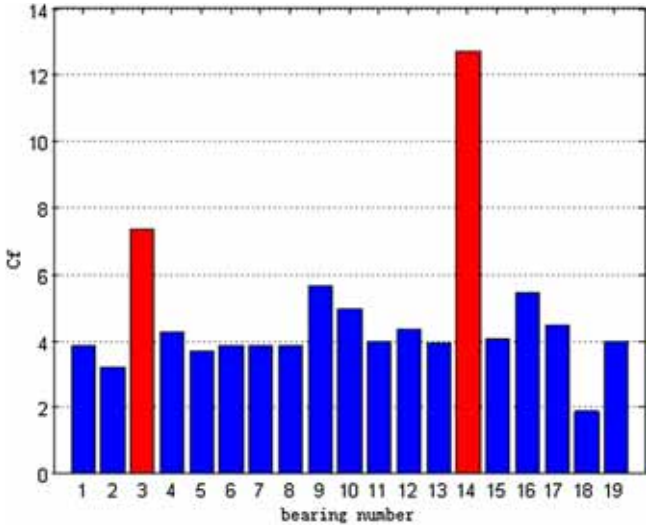

FIGURE 7 Crest factor (Cf) of the generator bearing vibration signal [Colour figure can be viewed at wileyonlinelibrary.com]

number 9 fault may not be detected by RMS. At the same time, three fault bearings are missed by kurtosis, even the serious fault bearing number 18. The threshold of CF is set to 6, and only two bearings' CF is greater than the threshold. Therefore, CF has low sensitiveness in generator bearing CM.

The ECI of the generator bearing vibration signal is displayed in Figure 8. The enlarged *Y* axis limit of ECI is shown in Figure 9 for details. Figures 8 and 9 indicate that three bearings are in alarm band and that five bearings are in warning band. Bearing number 9, which is regarded as health condition by RMS, is reported fault by ECI. Further analysis is performed to the vibration signal of bearing number 9 to assess the CM result.

Bearing number 9 is SKF6330C3/VL2071 deep groove ball bearing. It is located at the drive end of the generator. The rotating speed of the generator shaft during the test is 1406 rpm (Fr = 23.43 Hz). The calculated bearing defect characteristic frequencies, fundamental train frequency (FTF), ball spin frequency (BSF), BPFO, and ball pass frequency of the inner race (BPFI) of the bearings are given in Table 1.

The analysis result of bearing number 9 is shown in Figure 10. It shows that the periodic impulsive component is presented in the time waveform (Figure 10A), and the high-frequency resonance component can be found in the spectrum (Figure 10B), which indicate that bearing fault occurs. The characteristic frequency BPFI and its second harmonic, side frequency (BPFI ± Fr), which indicate the modulation feature of the bearing inner race fault, are clearly observed in the envelop spectrum (Figure 10C). The frequency 82.81 Hz and its second harmonic, which is very close to the theoretical BPFO characteristic frequency, are also clearly observed. Thus, the inner race fault and outer race fault are detected for this bearing.

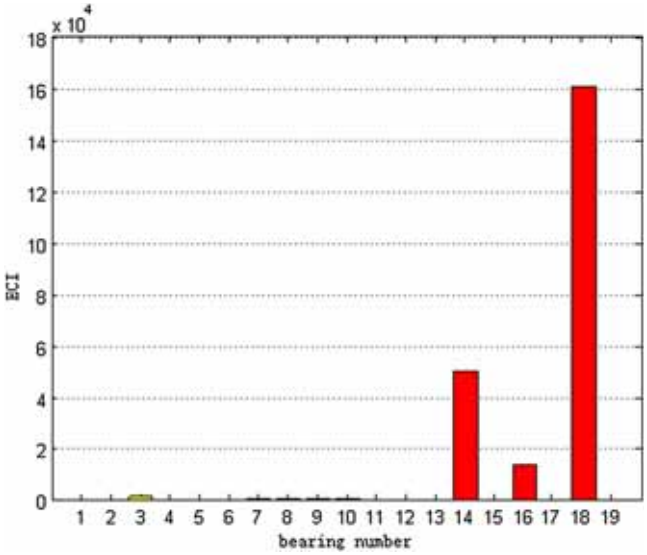

FIGURE 8 Engineering condition indicator (ECI) of the generator bearing vibration signal [Colour figure can be viewed at wileyonlinelibrary.com]

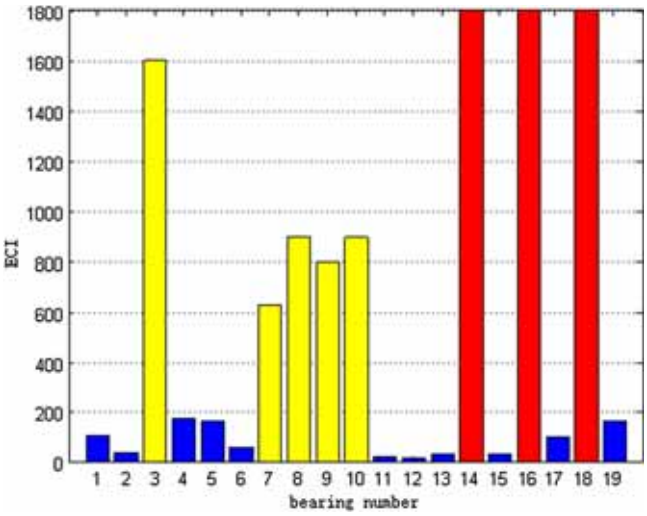

FIGURE 9 Details of engineering condition indicator (ECI) [Colour figure can be viewed at wileyonlinelibrary.com]

TABLE 1 Characteristic frequencies

FTF, Hz	BSF, Hz	BPFO, Hz	BPFI, Hz
9.35	55.4	84.1	126.8

Abbreviations: BPFI, ball pass frequency of the inner race; BPFO, ball pass frequency of the outer race; BSF, ball spin frequency; FTF, fundamental train frequency.

The result demonstrates that the ECI can give correct alarm in the CM and that it is more sensitive than the RMS.

5.3 | Application in gearbox bearing

The following vibration data are collected from a 1.5-MW DFIG wind turbines gearbox. The gearbox is composed of one low-speed (LS) planetary stage and two parallel stages, as shown in Figure 11. The planet carrier (PLC), LS shaft (LS-SH), intermediate-speed shaft (IMS-SH), and high-speed shaft (HS-SH) are marked by I, II, III, and IV in the figure, respectively.

The vibration test is performed in the nacelle with an accelerometer installed on the top of the gearbox close to the high-speed shaft. The sampling frequency is set to 12 800 Hz. VDI 3834 recommends that the acceleration warning and alarm limit guide value of gearbox in RMS are 7.5

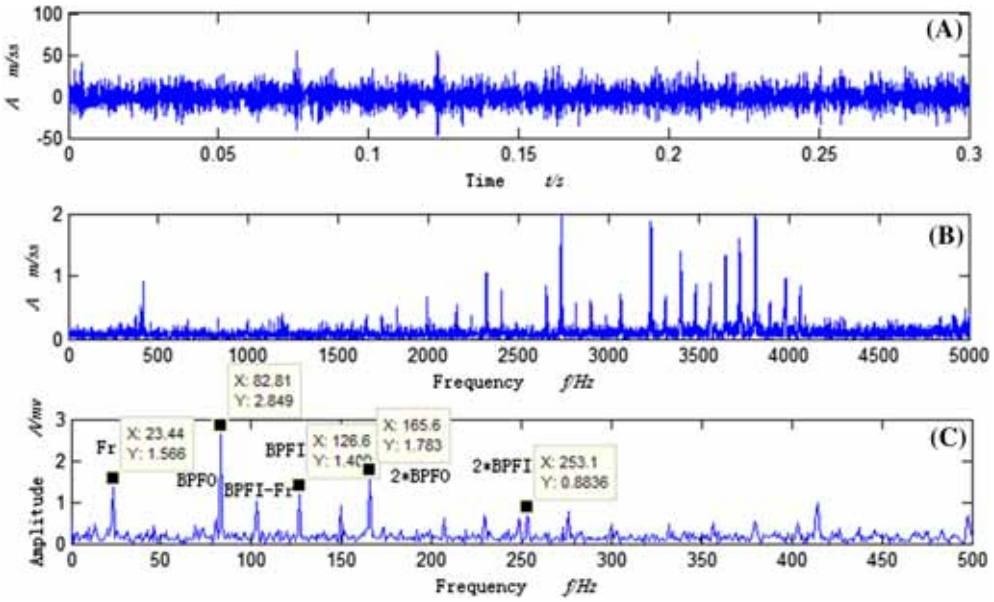

FIGURE 10 Analysis result of bearing number 9: A, time waveform; B, fast Fourier transform (FFT) spectrum; C, envelop spectrum [Colour figure can be viewed at wileyonlinelibrary.com]

and 12 m/ss, respectively. The limits are usually plus 25% of the guide values in engineering in China wind farm CM. The RMS value of the original vibration signal is 5.85 m/ss, which is lower than the guide value 7.5 m/ss of VDI 3834. According to the RMS warning limit, the gearbox is healthy. But abnormal condition is reported by ECI. The measurement result and threshold are supplied in Table 2. It shows the measured ECI value is about twice of the warning threshold. Figure 12 depicts the original vibration signal. Significant periodic impulsive component can be found in the time waveform, and the impulsive component period is estimated to be 0.176 seconds (5.68 Hz) from Figure 12B. The impulsive component has relative high peak value, but only a few bursts appear in 1 second. RMS is not significantly affected by these short bursts. The spectrum of the vibration signal is complicated, and high-amplitude components are mainly presented under 1500 Hz in Figure 13A. Calculation of gear ratio shows that the rotating frequency of IMS-SH is 5.73 Hz (1*X*), the IMS-SH gear meshing frequency is 131.85 Hz, and the HS-SH gear meshing frequency is 539.60. The IMS-SH gear meshing frequency and its harmonics are observed with abundant 1*X* sidebands in the spectrum (Figure 13B). The HS-SH gear meshing frequency is not found. The IMS-SH rotating frequency and its multiple harmonics are presented in the

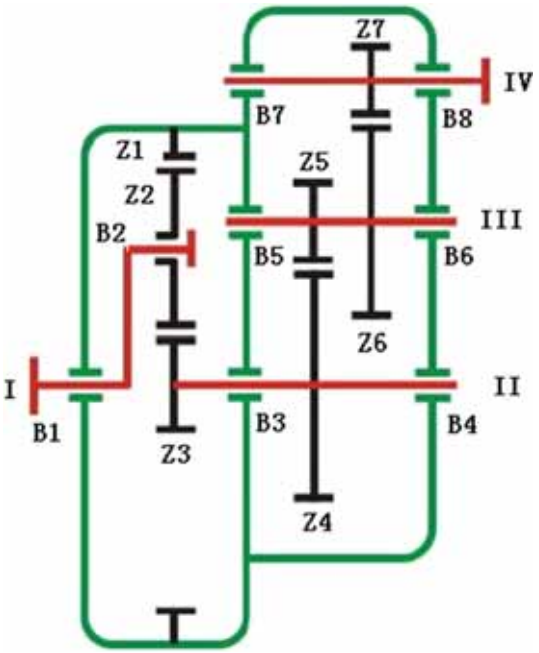

FIGURE 11 Diagram of the 1.5-MW wind turbines gearbox [Colour figure can be viewed at wileyonlinelibrary.com]

TABLE 2 Limits and measurement result

CIs	Warning Limit	Alarm Limit	Measurement Result
RMS	9.375	15	5.85
ECI	351.56	900	685

Abbreviations: CIs, condition indicators; ECI, engineering condition indicator; RMS, root mean square.

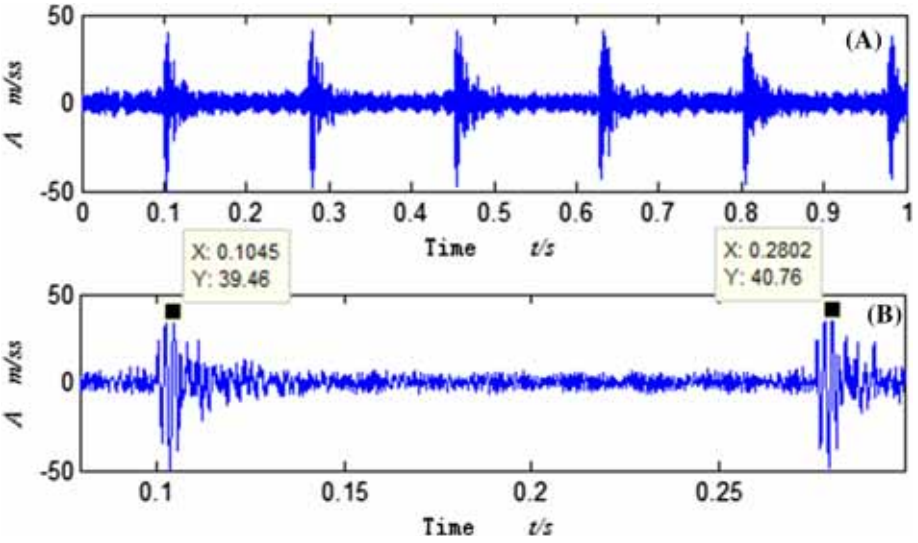

FIGURE 12 Gearbox vibration signal: A, time waveform; B, enlarged view [Colour figure can be viewed at wileyonlinelibrary.com]

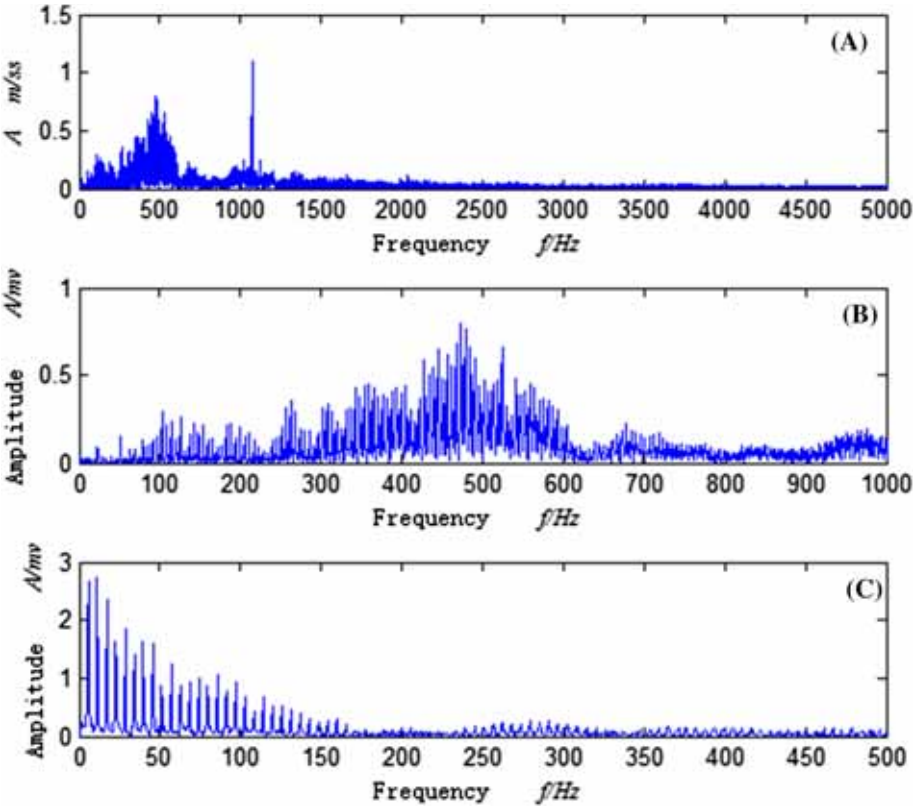

FIGURE 13 Gearbox vibration signal: A, fast Fourier transform (FFT) spectrum; B, local FFT spectrum; C, envelop spectrum [Colour figure can be viewed at wileyonlinelibrary.com]

envelop spectrum (Figure 13C). It seems that the cracked or broken tooth fault occurs on the pinion gear of the IMS-SH. However, the abundant harmonics (above 20*X*) and the noise floor in the spectra show evidence for a rotating looseness fault. In addition, loud periodic impacting sounds can be heard during the field test. These impacting sounds are compliant with quite obvious impacting property in the time waveform. Thus, the bearing looseness combined with gear tooth fault can be detected, but the periodic impacting is mainly caused by bearing looseness fault in the IMS-SH.

6 | CONCLUSION

CIs play a significant important role in wind turbine CM. Usually, further analyses or advanced signal processing techniques are implemented only when CI value passed the threshold levels. CIs for wind turbine bearing are reviewed. The advantages and disadvantages of these indicators are also discussed. From the aspect of wind turbine bearings engineering CM, a new ECI is proposed. The ECI has definite physical meaning, and it is the comprehensive representation of energy and kurtosis of the vibration signal. Quantitative thresholds of the ECI in wind turbine CM can be set according to the existing standard. The ECI can evaluate the overall condition and sensitive to incipient fault of wind turbine bearing. The bearing run-to-failure experiment data and a certain amount of field vibration test data of wind turbine demonstrate the effectiveness of ECI. Some faults, which are not indicated by general method, can be found by the proposed ECI. It is helpful for the accurate diagnosis of wind turbine bearing fault.

ACKNOWLEDGEMENT

This work was supported by the National Natural Science Foundation of China (grant nos. 51675178 and 51475164).

ORCID

Aijun Hu https://orcid.org/0000-0003-2844-671X

REFERENCES

1. http://www.wwindea.org/information2/information/
2. Soua S, Van Lieshout P, Perera A, Gan TH, Bridge B. Determination of the combined vibrational and acoustic emission signature of a wind turbine gearbox and generator shaft in service as a pre-requisite for effective condition monitoring. *Renew Energy*. 2013;51(2):175-181.
3. Sheng S. Wind Turbine Gearbox Condition Monitoring Round Robin Study—Vibration Analysis, Technical Report, NREL/TP-5000-54530, 2012
4. de Azevedo HDM, Araújo AM, Bouchonneau N. A review of wind turbine bearing condition monitoring: state of the art and challenges. *Renew Sustain Energy Rev*. 2016;56:368-379.
5. Márquez FPG, Tobias AM, Pérez JMP, et al. Condition monitoring of wind turbines: techniques and methods. *Renew Energy*. 2012;46:169-178.
6. Liu WY, Tang BP, Han JG, Lu XN, Hu NN, He ZZ. The structure healthy condition monitoring and fault diagnosis methods in wind turbines: a review. *Renew Sustain Energy Rev*. 2015;44:466-472.
7. Kabir MJ, Oo AMT, Rabbani M. A brief review on offshore wind turbine fault detection and recent development in condition monitoring based maintenance system. Power Engineering Conference (AUPEC), 2015 Australasian Universities. IEEE, 2015: 1–7.
8. Feng Y, Qiu Y, Crabtree CJ, Long H, Tavner PJ. Monitoring wind turbine gearboxes. *Wind Energy*. 2013;16(5):728-740.
9. Yang W, Tavner PJ, Crabtree CJ, Feng Y, Qiu Y. Wind turbine condition monitoring: technical and commercial challenges. *Wind Energy*. 2014;17(5):673-693.
10. Wymore ML, Van Dam JE, Ceylan H, et al. A survey of health monitoring systems for wind turbines. *Renew Sustain Energy Rev*. 2015;52:976-990.
11. Purarjomandlangrudi A, Nourbakhsh G, Esmalifalak M, Tan A. Fault detection in wind turbine: a systematic literature review. *Wind Engineering*. 2013;37(5):535-547.
12. Spinato F, Tavner PJ, Van BGJW, Koutoulakos E. Reliability of wind turbine subassemblies. *IET Renew Power Generation*. 2009;3(4):1-15.
13. Gray C, Watson S. Physics of failure approach to wind turbine condition based maintenance. *Wind Energy*. 2010;13(5):395-405.
14. Liancheng S, Xinglin L, Wang W, et al. Investigation and analysis of fault for wind turbine bearings in northern China. *Bearings*. 2011;11:59-62. (in Chinese)
15. Tang BP, Song T, Li F, Deng L. Fault diagnosis for a wind turbine transmission system based on manifold learning and Shannon wavelet support vector machine. *Renew Energy*. 2014;62:1-9.
16. Wang J, Gao R, Yan R. Integration of EEMD and ICA for wind turbine gearbox diagnosis. *Wind Energy*. 2013;17:757-773.
17. Zhipeng F, Liang M. Complex signal analysis for wind turbine planetary gearbox fault diagnosis via iterative atomic decomposition thresholding. *J Sound Vib*. 2014;333:5196-5211.
18. Sheng S. Investigation of oil conditioning, real-time monitoring and oil sample analysis for wind turbine gearbox. AWEA Project Performance and Reliability Workshop 2011;
19. Lu S, Zheng P, Yongbin L, et al. Sound-aided vibration weak signal enhancement for bearing fault detection by using adaptive stochastic resonance. *J Sound Vib*. 2019;449:18-29.
20. Yang W, Court R, Jiang J. Wind turbine condition monitoring by the approach of SCADA data analysis. *Renew Energy*. 2013;53:365-376.

21. Guo P, Bai N. Wind turbine gearbox condition monitoring with AAKR and moving window statistic methods. *Energies*. 2011;4(11):2077-2093.
22. Hameed Z, Hong YS, Choa YM, Ahn SH, Song CK. Condition monitoring and fault detection of wind turbines and related algorithms: a review. *Renew Sustain Energy Rev*. 2009;13(1):1-39.
23. Yang W, Tavner PJ, Tian W. Wind turbine condition monitoring based on an improved spline-kernelled Chirplet transform. *IEEE Trans Ind Electron*. 2015;62(10):6565-6574.
24. Antoniadou I, Manson G, Staszewski WJ, Barszcz T, Worden K. A time–frequency analysis approach for condition monitoring of a wind turbine gearbox under varying load conditions. *Mech Syst Signal Process*. 2015;64:188-216.
25. Zimroz R, Bartelmus W, Barszcz T, Urbanek J. Diagnostics of bearings in presence of strong operating conditions non-stationarity—a procedure of load-dependent features processing with application to wind turbine bearings. *Mech Syst Signal Process*. 2014;46(1):16-27.
26. Zhu J, Nostrand T, Spiegel C, Morton B. Survey of condition indicators for condition monitoring systems[C]//Annu. Conf Progn Heal Manag Soc 2014, 5: 1–13.
27. Igba J, Alemzadeh K, Durugbo C, Eiriksson ET. Analysing RMS and peak values of vibration signals for condition monitoring of wind turbine gearboxes. *Renew Energy*. 2016;91:90-106.
28. Goyal D, Pabla BS, Dhami SS. Condition monitoring parameters for fault diagnosis of fixed axis gearbox: a review. *Archives Computational Meth Eng*. 2016;24:1-14.
29. Kandukuri ST, Klausen A, Karimi HR, Robbersmyr KG. A review of diagnostics and prognostics of low-speed machinery towards wind turbine farm-level health management. *Renew Sustain Energy Rev*. 2016;53:697-708.
30. Večeř P, Kreidl M, Šmíd R. Condition indicators for gearbox condition monitoring systems. *Acta Polytechnica*. 2005;45(6):35-43.
31. Batista L, Badri B, Sabourin R, Thomas M. A classifier fusion system for bearing fault diagnosis. *Expert Systems with Applications*. 2013;40(17):6788-6797.
32. Immovilli F, Bianchini C, Cocconcelli M, Bellini A, Rubini R. Bearing fault model for induction motor with externally induced vibration. *IEEE Trans Ind Electron*. 2013;60(8):3408-3418.
33. Yu J. Local and nonlocal preserving projection for bearing defect classification and performance assessment. *IEEE Trans Ind Electron*. 2012;59(5):2363-2376.
34. Sassi S, Badri B, Thomas M. Tracking surface degradation of ball bearings by means of new time domain scalar indicators. *Int J Comadem*. 2008;11(3):36-45.
35. Qiu H, Lee J, Lin J. Wavelet filter-based weak signature detection method and its application on roller bearing prognostics. *J Sound Vib*. 2006;289(4-5):1066-1090.
36. Wang D, Shen C. An equivalent cyclic energy indicator for bearing performance degradation assessment. *J Vib Control*. 2014;22(10):2380-2388. https://doi.org/10.1177/1077546314547224

How to cite this article: Hu A, Xiang L, Zhu L. An engineering condition indicator for condition monitoring of wind turbine bearings. *Wind Energy*. 2019;1–13. https://doi.org/10.1002/we.2423